Evidence of a Threshold Wind Speed in Tower-mounted Scatterometer Data

David W. Draper and David G. Long
Brigham Young University, Microwave Earth Remote Sensing Laboratory
459 CB, Provo, UT 84602 801-378-4884, FAX: 801-378-6586 draperd@ee.byu.edu, long@ee.byu.edu

***Abstract*- The normalized radar backscatter (σ^o) in scatterometer measurements over water is theorized to go to zero below a threshold wind speed due to insufficient friction between the wind and water to create capillary waves from which the radar signal scatters. Evidence of the threshold wind speed and a hysteresis effect have been observed in airship and wave tank data. The threshold wind speed is additionally evidenced in tower-mounted scatterometer data in an uncontrolled marine environment. *In situ* wind measurements and corresponding σ^o values obtained from YSCAT, an ultra-wideband scatterometer deployed on the Canada Centre for Inland Waters research tower at lake Ontario, are used to detect and estimate the threshold wind speed. A detectable threshold is evidenced in approximately 1/2 of the observations. The observed threshold wind speeds correspond well to theoretical threshold wind speeds.**

I. Introduction

Measuring marine winds is the fundamental application of scatterometer data. Scatterometers infer ocean winds by measuring the normalized radar backscatter cross-section (σ^o) of the ocean surface. The backscatter is related to the near-surface wind speed and direction due to Bragg scattering from wind-generated capillary waves. The wind is inferred via an empirical relationship between the wind and σ^o, known as the Geophysical Model Function (GMF). The GMF is generally accurate for wind speeds above about 3 to 4 m/s. At lower wind speeds, Donelan and Pierson postulated the existence of a threshold wind speed below which there is insufficient friction between the wind and water to generate capillary waves [1]. The Bragg-induced backscatter below the threshold wind speed theoretically goes to zero. The threshold is highly dependent on Bragg wavelength and has been documented in airship data [2].

YSCAT, an ultra-wideband (2-14 GHz) tower-mounted scatterometer, provides significant evidence of the threshold wind speed in an uncontrolled marine environment. YSCAT was deployed on Lake Ontario for a period of 6 months in 1994 [3]. Data was collected for a variety of frequencies and incidence angles which span a range of Bragg wavelengths. This paper examines the YSCAT data for evidence of a threshold wind speed as a function of Bragg wavelength. A simple experiment is conducted in which approximately 1/2 of the Bragg wavelengths observed by YSCAT evidence a threshold wind speed. The estimated threshold corresponds well to the theoretical threshold for both h-pol and v-pol data.

II. Background

YSCAT collected data at 2, 3, 5, 10, and 14 GHz, and at 0° (nadir), 20°, 25°, 30°, 40°, 50°, and 60° incidence angles at both horizontal and vertical polarizations. In addition, a variety of environmental parameters were observed including wind speed and direction, rainfall, and water temperature. The antenna was specially designed to provide a near constant beam width over most of the operating bandwidth and produce a footprint of approximately one meter for mid-range incident angles [3].

Post processing of YSCAT data provides minute averages of σ^o and *in situ* measurements of wind velocity. Rain-contaminated data, data corrupted by instrument malfunctions or other sources of error, and data with fluctuating wind speed measurements are discarded. The minute-averaged data is binned according to frequency, polarization, incidence angle, and direction. Data is additionally binned into upwind and downwind directions. The data is normalized by dividing out the mean of each record and then multiplying by the aggregate mean of the corresponding bin [3].

The large number of frequencies and incidence angles provides a wide range of Bragg wavelengths observed by the YSCAT instrument. The Bragg wavelength is the component of the water wave spectrum that is resonant with the incident frequency. A first order Bragg theory analysis (used in this paper) relates the Bragg wavelength Λ to the electromagnetic wavelength λ by

$$\Lambda = \frac{\lambda}{2\sin(\theta)} \tag{1}$$

where θ is the incidence angle. The wide range of Bragg wavelengths observed by YSCAT affords us access to understanding the wind/sea interaction for a large number of wave sizes. The Bragg wavelengths measured by YSCAT range from 1.2 cm to 43 cm.

III. Theoretical Threshold Wind Speeds

The theoretical threshold wind speed is derived in [1]. At low wind speeds, friction from the wind is too light to overcome the viscous effects of water and no capillary/gravity waves are generated. If we accept Bragg scattering as the predominate scattering mechanism, under these conditions, there should be no backscatter at all [4]. The threshold wind speed at $\pi/k = \lambda/2$ height is derived to be [1]

$$\bar{U}(\pi/k) = C(k) + 2\left(\nu k \frac{C(k)}{0.194\rho_a/\rho_w}\right)^{1/2}. \tag{2}$$

In Eq. 2, $C(k)$, the phase speed of the capillary/gravity Bragg waves, is given by

$$C(k) = \sqrt{g/k + \tau k/\rho_w}. \tag{3}$$

TABLE I

THEORETICAL THRESHOLD WIND SPEEDS (M/S) AS A FUNCTION OF FREQUENCY AND INCIDENCE ANGLE FOR YSCAT

Frequency (GHz)	Incidence Angle						
	10°	20°	25°	30°	40°	50°	60°
2.00	1.98	1.94	1.95	1.98	2.03	2.09	2.14
3.05	1.93	1.99	2.03	2.09	2.19	2.28	2.36
5.30	1.96	2.15	2.26	2.36	2.55	2.72	2.87
10.02	2.14	2.56	2.77	2.98	3.40	3.79	4.12
14.00	2.30	2.92	3.24	3.57	4.23	4.85	5.40

Also, ρ_a and ρ_w are the densities of air and water respectively, τ is the surface tension, g is the acceleration of gravity, and ν is the viscosity of water. The viscosity has a dependence on water temperature. Thus, the threshold wind speed is a function of Bragg wavelength and temperature. It is also a weak function of salinity, which is ignored here. The wind speed at π/k height is related to the wind speed at 10 m height by the equation

$$\bar{U}(\pi/k) = \bar{U}(10)\left(1 - \frac{[A + B\bar{U}(10)]^{1/2}}{\kappa}[\ln k - \ln(\pi/10)]\right) \quad (4)$$

where A = $0.96e^{-3}$, B = $0.041e^{-3}$, and κ is the von Karman constant assumed to be 0.4. The threshold wind speed at 10m ($\bar{U}(10)$) must be numerically solved for. The theoretical threshold wind speeds for YSCAT at 10° C water temperature are given in Table I.

A. Detection and Estimation of YSCAT Threshold Wind Speeds

A simple experiment is performed to detect and estimate the threshold wind speed versus Bragg wavelength using YSCAT data. Assuming that downwind and upwind observations exhibit the same threshold characteristics, downwind and upwind measurements are combined in the analysis. The backscatter cross-section above the threshold wind speed (which we initially approximate as 4 m/s) has a power-law relationship with wind speed[3],

$$\sigma^\circ(U > \bar{U}(10)) = aU^b. \quad (5)$$

Using YSCAT minute average wind speeds and σ° values, the parameters a and b for each Bragg wavelength are computed for wind speeds above 4 m/s by converting both sides of Eq. 5 to decibels,

$$\sigma^\circ_{\text{dB}} = a_{\text{dB}} + bU_{\text{dB}} \quad (6)$$

and applying linear least-squares estimation to the YSCAT data [3]. After estimating a_{dB} and b, all σ° values further than 2 standard deviations from the model fit are discarded. The estimation is then performed again, giving the final values for a_{dB} and b.

Next, non-parametric estimation is performed on each Bragg wavelength data set using a Gaussian kernel. This method gives a smoothed line through the data relating U_{dB} and σ°_{dB}. The non-parametric curve affords a higher resolution estimate of the data than the linear least-squares fit.

In order to select a threshold wind speed for each Bragg wavelength data set, we compare the non-parametric curve to the linear least-squares fit. Since the data is obtained from an uncontrolled marine environment and is minute-averaged for each observation, we do not expect the σ° values to go to zero below the threshold wind speed, but we do expect σ° to decrease in mean value and have a higher variability. We estimate the threshold wind speed to be the point where the non-parametric curve falls 1.5 dB (25%) beneath the linear least-squares fit. The threshold of 1.5 dB is subjectively chosen, but the results are not particularly sensitive to this value. If the curve *never* falls 1.5 dB beneath the linear fit, we label the data a "non-detection" (N/D).

Using this method, 20 of the 35 data Bragg wavelength bins observed by YSCAT have a detectable threshold wind speed for h-pol observations. Of the fifteen non-detections, 4 sets exhibit a noticeable noise floor that prevents observation of the threshold wind speed. In addition, one set has no usable data.

Of the v-pol observations, 16 sets have a detectable threshold wind speed. Of the nineteen non-detections, seven sets exhibit a noticeable noise floor and one set contains no usable data. The v-pol data is much noisier than the h-pol data, thus giving a higher variance in the estimates of the wind speed threshold and possibly prohibiting detection in some cases.

The theoretical threshold wind speeds are plotted along with the results obtained from this experiment in Fig. 1. Also in Fig. 1, a second-order polynomial fit is made to the h-pol and v-pol thresholds. Both polynomial fits give a close approximation of the thresholds in the range of valid detections. The v-pol data is slightly more variable than the h-pol data, giving a fit that

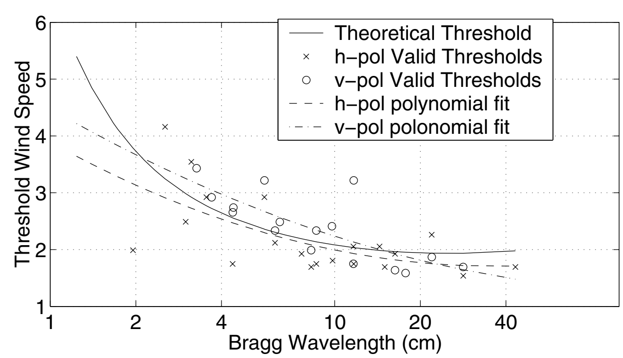

Fig. 1. The theoretical threshold wind speeds for the range of Bragg wavelengths observed by YSCAT. Also, the estimated threshold wind speeds for v-pol and h-pol observations obtained from the YSCAT data where a threshold wind speed is detected. The dashed and dot-dashed lines show a second order polynomial fit to the h-pol and v-pol threshold wind speeds respectively.

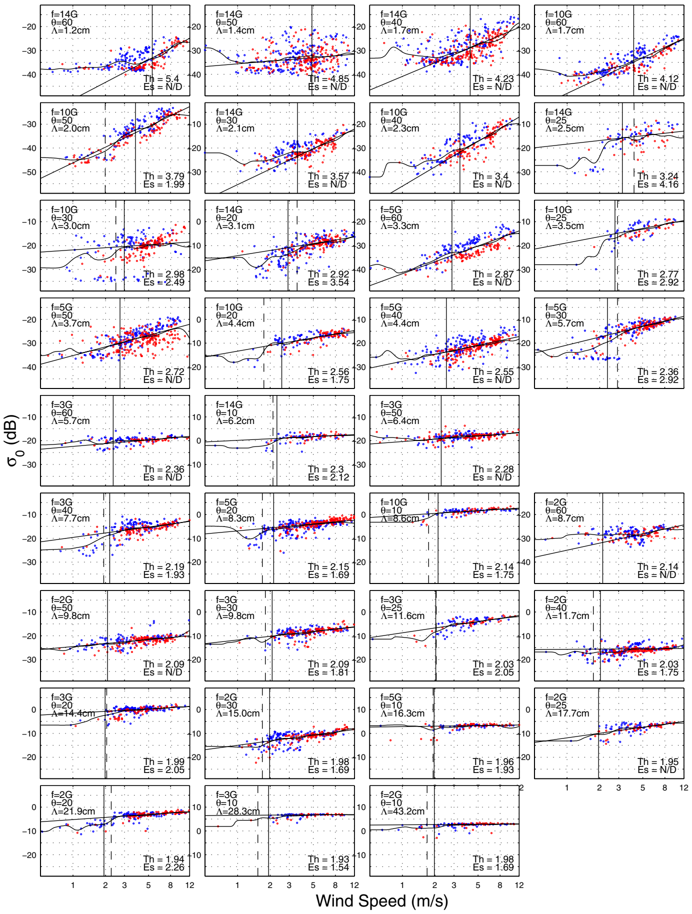

Fig. 2. H-pol YSCAT data plotted as a function of wind speed for each Bragg wavelength. The straight line through the data is the linear least-squares fit. The curved line is the non-parametric fit. The solid vertical line is the theoretical threshold wind speed (Th). The dashed line is the threshold wind speed estimated from the YSCAT data (Es).

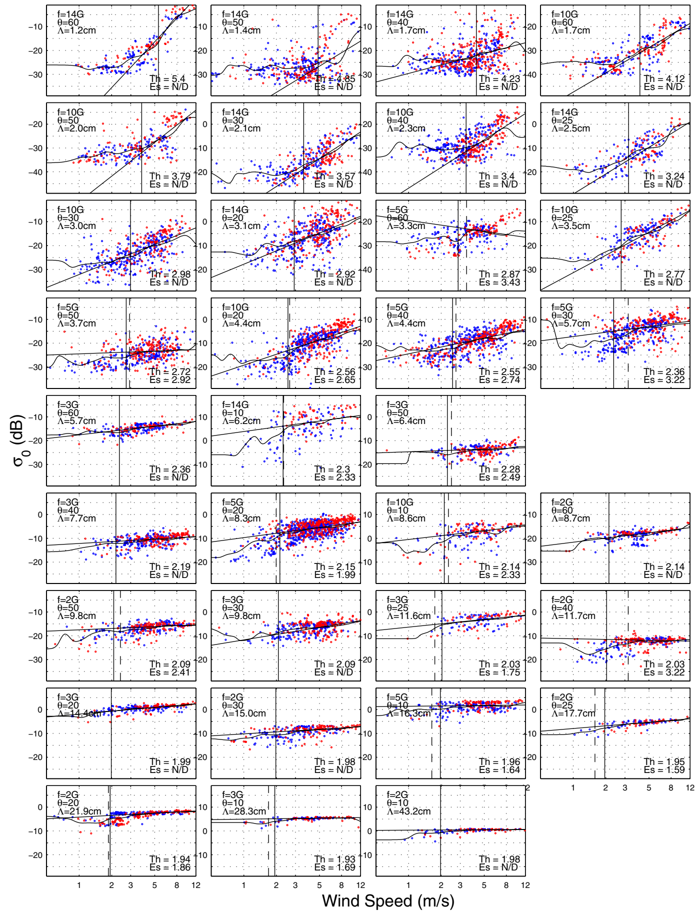

Fig. 3. V-pol YSCAT data plotted as a function of wind speed for each Bragg Wavelength and polarization (See Fig. 2).

deviates more from the theoretical thresholds. These results help verify the existence of the threshold wind speed, and give support to the accuracy of the model.

The YSCAT data along with the theoretical and estimated threshold wind speeds are shown in Fig. 2 and 3. These figures allow for visualization of the threshold wind speed and resulting drop in σ°. As illustrated in Fig. 2 and 3, the roll-off in σ° below the threshold is not as pronounced as in controlled wave tank data where the signal drops nearly to zero. Nevertheless, YSCAT data suggests that for small-footprint instruments, effects of the threshold wind speed are detectable in an uncontrolled environment.

IV. Conclusions

YSCAT data demonstrates strong evidence of a threshold wind speed in an uncontrolled marine environment. The experiment in this paper demonstrates that in approximately 1/2 of the YSCAT Bragg wavelength observations, a detectable roll off in σ° is evident beneath a threshold wind speed. The YSCAT-estimated threshold wind speeds correspond well to the theoretical threshold wind speeds derived by [1], and help support the theory of a threshold wind speed.

References

[1] M. A. Donelan and W. J. Pierson, "Radar scattering and equilibrium ranges in wind generated waves with application to scatterometry," *Journal of Geophysical Research*, vol. 92, no. C5, pp. 4971-5029, May 1987.

[2] W. J. Plant, W. C. Keller, V. Hesany, K. Hayes, K. W. Hoppel, and T. V. Blanc, "Measurements of the marine boundary layer from an airship," *Journal of Atmospheric and Oceanic Technology,* vol. 15, no. 6, pp. 1433-1458, Dec 1998.

[3] D. G. Long, R. S. Collyer, R. Reed, and D. V. Arnold, "Dependence of the Normalized Radar Cross Section of Water Waves on Bragg Wavelength-Wind Speed Sensitivity," *IEEE Transactions on Geoscience and Remote Sensing*, vol. 34, no. 3, pp. 656-666, May 1996.

[4] K. Shankaranarayanan and M. A. Donelan, "A probabilistic approach to scatterometer model function verification," *Journal of Geophysical Research,* vol. 106, no. C9, pp. 19,969-19,990, Sep. 2001.